論文 79 - 16 - 6 - 4

Resolution Improvement of the Positron Computerized Tomography with a New Positron Camera Tomographic System
(分解能 向上을 爲한 새로운 陽電子 斷層 撮影機의 提案)

洪 起 祥*, 羅 鍾 範**

(Hong, Ki Sang and Ra, Jong Beom)

要 約

새로운 構造의 陽電子 電算 斷層 撮影機(Positron Computerized Tomography)를 提案하고 그 시스템의 性能을 컴퓨터로 예측하였다. 이 새로운 構造의 시스템은 sampling 간격을 임의로 할 수 있기 때문에 既存의 시스템에 비해서 보다 높은 分解能의 斷層 影像을 얻을 수 있다. 컴퓨터 시뮬레이션으로 이 시스템에 어떠한 artifact가 생기나 살펴 보았고 Poisson noise가 더해졌을 때의 影像을 比較함으로써 이 시스템이 既存의 시스템보다 나은 影像을 얻을 수 있음을 確認하였다.

Abstract

A new circular ring positron camera tomographic system termed "Oscillatory Dichotomic Ring" system is proposed and its performance is simulated. It is basically a circular ring system, composed of two half rings, which has the capability of scanning so that any sampling intervals can be obtained. Since finer sampling means poorer photon statistics, simulations with various signal dependent statistical noise effects, ray sampling and arrangement as well as related artifacts peculiar to the proposed Dichotomic Ring system are made.

I. Introduction

Since the concept of imaging positron emitting radionuclides was first suggested by Brownell,[1] there has been considerable research and advancement particularly in the direction of 3-D tomographic systems.[2, 3] There were some problems related to tomographic systems using positron annihilation coincident techniques such as low statistics, inadequate computational hardware and algorithms, and data distortion from photon attenuation effects etc. Many of the problems remained unsolved until the EMI XCT (X-ray Computerized Tomography) system was first developed by Hounsfield[4] in 1972. This stimulated the development of ECT (Emission Computerized Tomography) which resulted in the first practical positron emission CT PETT III developed by Ter-Pogossian and Phelps at Washington University in 1974-1975,[5] which obtains data using scanning motion. Following PETT III, a circular ring transaxial positron camera (CRTAPC I) was developed by Z.H. Cho et al.[6] at UCLA aiming at more efficient

*準會員, 韓國科學院 電氣 및 電子工學科
(Dept. of Electrical Science, KAIS)

**正會員, 光云工大 電子工學科
(Kwangwoon Institute of Technology)

接受日字 : 1979年 11月 2日

and faster coincident data collection in a stationary manner.

However, a stationary ring system suffers from insufficient number of sampling rays which results in some loss of frequency response and spatial resolution. Several methods have been proposed to improve the ray sampling.

One method suggested by Cho et al.[6] is a rotation of the ring about its axis in increments equal to half the circumferential detector spacing which imrpoves the ray sampling by a factor of two, but this still does not meet the sampling requirement in which Nyquist sampling distance should be smaller than a quarter of the detector width.[7] Other methods such as Wobbling[8, 9] and Positology[10] have been suggested; the former describes the motion of a circular detector ring where the orientation stays fixed while the entire ring moves in a small circular path; the latter uses a continuously rotating positron ECT system in which the detectors are arranged on a circular ring with "non uniform" spacing so as to provide a finer sampling interval. In wobbling system, the detectors will give parallel ray data at all positions of the ring system. The limitations on this system are the size of the orbital path and the complexity of the mechanism to obtain this motion.

The new proposed system is an oscillating Dichotomic-Ring (DR) system which can provide the desired sampling interval with very simple motion. The description of the system structure, its characteristics and simulated performances will be presented. The simulation results including noise effects and other system-dependent limitations, and their solutions will also be discussed.

II. Proposed System Structure

Proposed Oscillating Dichotomic-Ring system differs from a conventional circular ring system in that it consists of two half ring detector arrays with one detector omitted at one end of each array. This means the system shapes into a circular ring with two detectors vacant at the opposite sites on the circular ring as shown in Fig. 1. Equal angular rotation of these two half rings in opposite directions within a distance equal to half detector width makes it possible to sample with any desired interval as illustrated in Fig. 1.

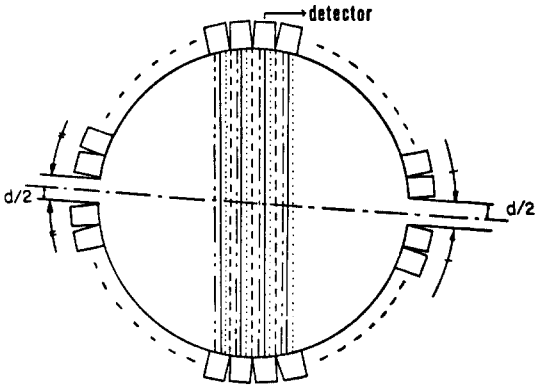

Fig. 1. Oscillatory Dichotomic-Ring System Arrows at both sides indicate the same angular rotation of the two half rings within the distance equal to half of detector width d. Lines indicate ray sampling at the position of d/4 rotation in one direction (— - - —), no rotation (——), d/4 (------), and d/2 (- - - -) rotation in the other direction, respectively.

As shown in Fig. 2, coincidence detections occurring at two detectors on the same half ring constitute parallel projection data only

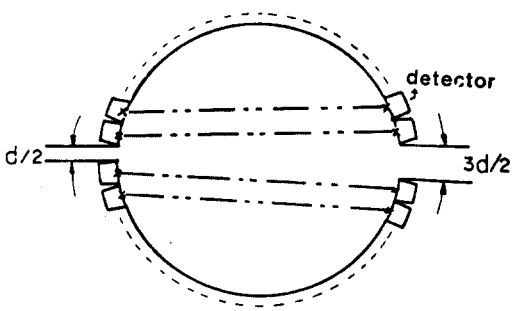

(a)

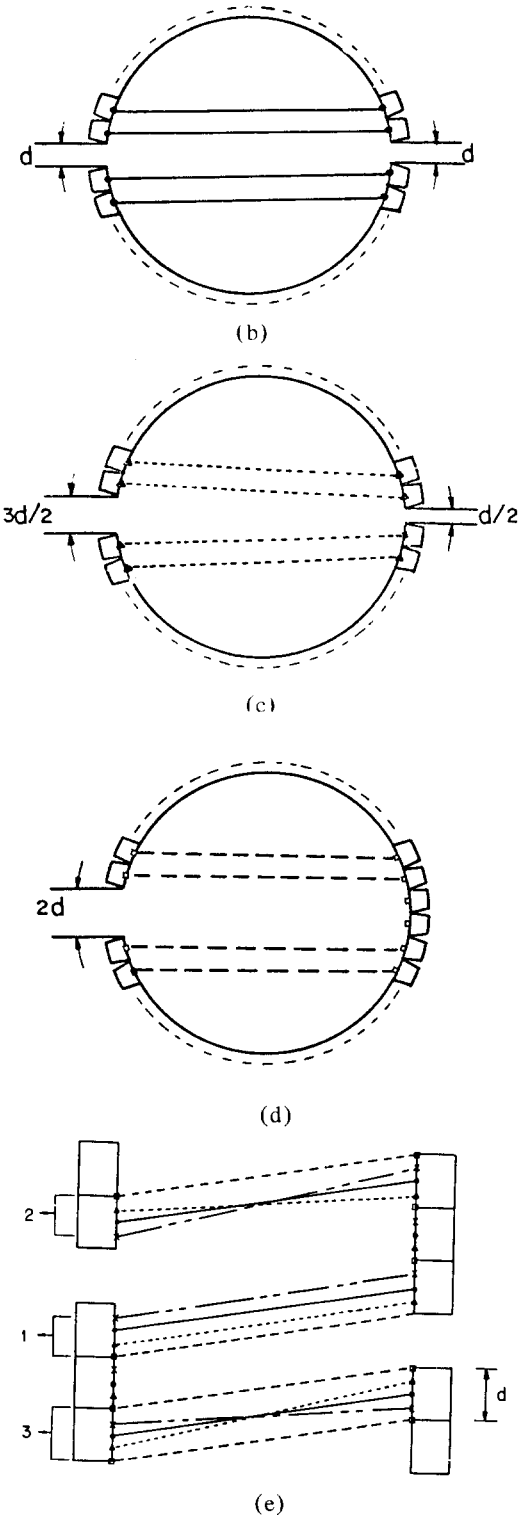

Fig. 2. (a) phase I
(b) phase II (=original position)
(c) phase III
(d) phase IV
(e) Schematic diagram of DR system near the junction of two half rings. Marks x, ○, △, □, denote center of detector at each rotated positions (a), (b), (c), and (d), respectively. Sequence of oscillating motion is as follows; phase II → III → IV → III → II → I → II. As shown in (e), coincidence detections occurring on the different half rings always constitute parallel rays (1), while those occurring on the same half ring (2, 3) do not, except at the positions of phase II and IV.

at the original (phase II) and half detector width rotated position (phase IV). At all other positions for detectors on the same half ring, the projection sets are not valid since the rays are non parallel (NP). On the other hand, coincidence data for detectors on opposite half rings are always parallel for all rotation positions. Therefore, coincidence detection obtained on the same half ring at the position other than the original and half detector width rotated should be discarded. Linear interpolation can be used to complement those discarded ray data and these interpolated data are used for the simulation to observe the artifact which might arise from the discard of these rays. Since the NP rays are discarded, there is some loss of valid photons. In addition, another loss occurs due to the vacancy of two detectors, which is needed for rotation of the two half rings. Estimates of these losses will be given in the following simulation results.

From the viewpoint of the signal dependent noise, assuming that finite amounts of the radionuclides are injected into the object within a given time, the photon statistics becomes poorer as the number of ray samples is increased. It was found that the image degradation due to data discard and linear interpolation

was insignificant when signal dependent noise is taken into account. These effects are demonstrated in the experimental computer simulations.

III. Experimental Results and Computer Simulations

Description of the simulated system structure is as follows;

Ring Diameter	: D_R = 60 cm
Object Diameter	: Do = 30cm
Detector Width	: d = 0.7 cm
Number of Detectors	: $N_D = D_R/d = 270$
Number of Views	: $N = N_D/2 = 135$
Number of Detectors within one view	: $M_O = D_O/d = 43$.

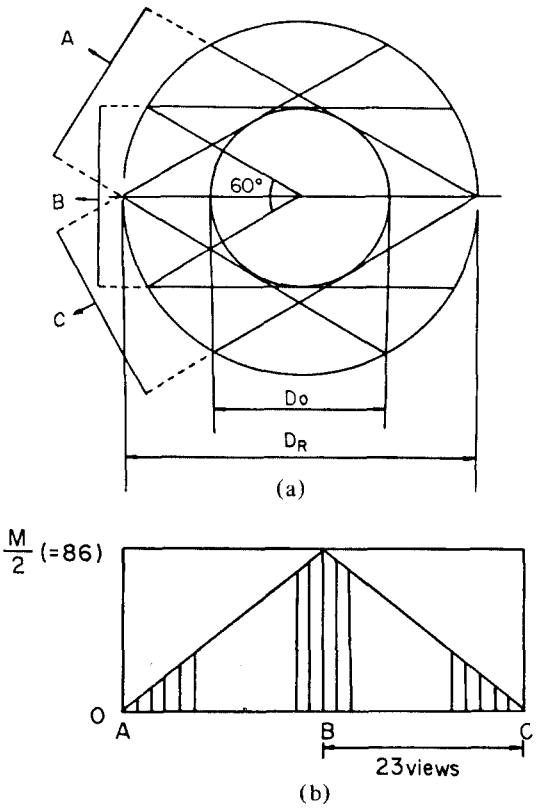

Fig. 3. Views containing non parallel rays are shown in (a). They occupy the portion of 60°. Total number of non parallel rays are shown in (b).

In this simulation, sampling interval is a quarter of a detector width so that the number of samples per view (M) becomes four times than that of the stationary case (M_O), that is,

$$M = 4 \times M_O = 172.$$

The loss due to NP rays and the vacancy of two detectors for the rotation of the two half rings stated earlier is now calculated roughly.

First, the loss due to invalid NP rays can be calculated as follows; The number of views containing NP rays is

$$N_W = N_D \times 60^\circ/360^\circ = 45 \text{ (views)}$$

so that the total number of rays in the above 45 views is

$$M_W = N_W \times M = 7{,}740 \text{ (rays)}$$

as shown in Fig. 3. Half of them are valid since rays sampled at the original and d/2 rotated position constitute the parallel projection data, while rays sampled at d/4 or 3d/4 rotated position do not. Of the another half, half of them are NP rays since the number of NP rays increases linearly from zero to M/2 (=86) between A and B and again decreases to zero from B to C. This linear increase is 4 rays per step as can be seen in Fig. 3, where the view B is parallel view with the diameter which connects the junctions of the two half rings. Therefore total number of NP rays is

$$M_{wt} = M_w \times 1/2 \times 1/2 = 1{,}935 \text{ (rays)}.$$

Second, the loss due to the vacancy of the two detectors is easily calculated so that the number of rays lost is

$$M_v = 2 \times 4 \times 90 = 720 \text{ (rays)},$$

where "2" is the number of vacant detector locations, "4" is number of samples per detector and "90" is the number of detectors which could be seen at the vacant site through the object. Total loss of rays then becomes

$$M_t = M_{wt} + M_v = 2{,}655 \text{ (rays)}.$$

If it were possible to sample with d/4 sampling

distance without any loss (ideal case), total number of rays would be

$$M_I = M \times N = 23{,}220 \text{ (rays)}.$$

Percent loss, therefore, can be written approximately

$$E_{Loss} = M_t/M_I \times 100 \text{ or } 11.4\%.$$

But exact calculation of the loss shows about 9.0% and this loss was found to be insignificant in the simulations.

The simulations were performed with HP3000, and the results were obtained through the line printer terminal.

Fig. 4 shows the brief flow chart of the used program.

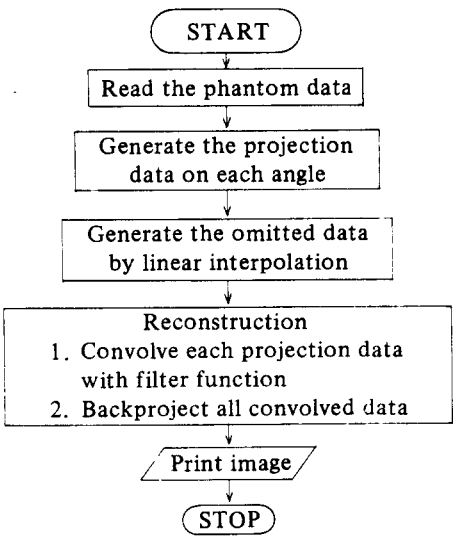

Fig. 4. The brief flow chart of the used program.

Fig. 5 shows the simulation phantom and its results for the case of 86 and 172 samples per view (M) in the ideal case and 172 for the Dichotomic-Ring system, where the ideal case means that the number of detectors are 4 times more than that of the Dichotomic-Ring system and that data is collected without any motion. There is no significant difference between the ideal and the Dichotomic-Ring in the case of M=172. Superiority of the Dichotomic-Ring system at the high sampling rate (4 times) to that of M=86, the original undersampled case, is obvious.

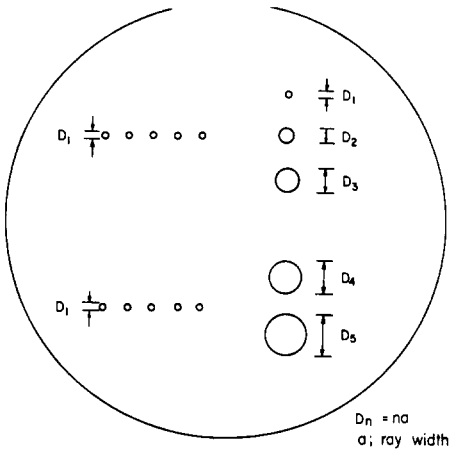

(a)

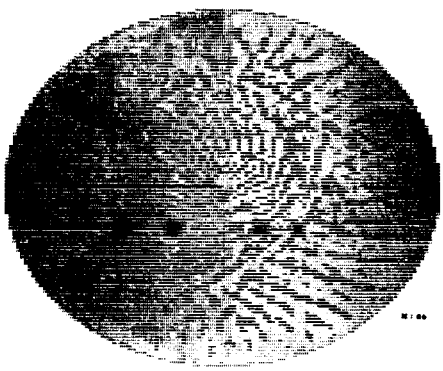

(b)

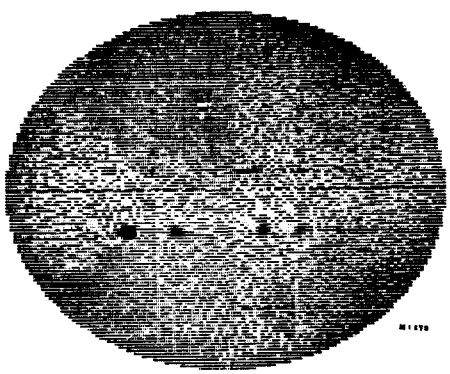

(c)

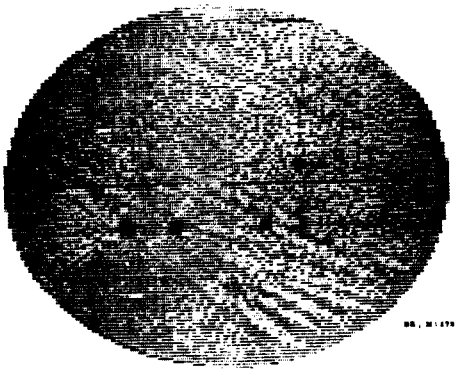

(d)

Fig. 5. (a) Simulation phantom, all the circles have the same contrast of 1.5 against background gray level which is fixed to 1.
(b) M=86, ideal case
(c) M=172, ideal case
(d) M=172, DR system
All the images are composed of 128 x 128 pixels.

Fig. 6 shows the simulations of a phantom and their results with the addition of Poisson signal dependent noise. Total number of photons collected by detectors is assumed to be about 11 million. This amounts to 1,000 photons per sampling when M=86, which means about 3.1% of noise. In the case of M=172 of the Dichotomic-Ring system, 500 photons are collected per sampling with the noise to signal ratio of about 4.5%.

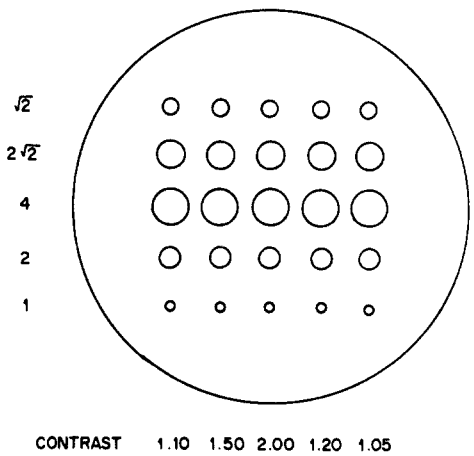

(a)

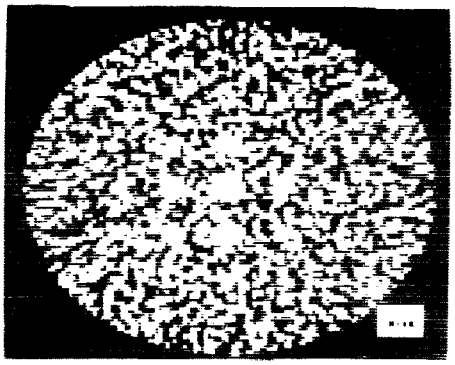

(b)

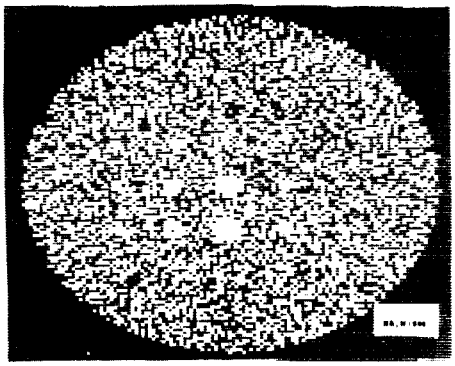

(c)

Fig. 6. (a) Simulation phantom
Numbers in the left side indicate the size of circles in each row, where unit 1 is equivalent to 2 pixels in diameter. Circles in the same column have the same contrast against background gray level which is fixed to 1.
(b) M=86, Number of photons per sampling =1,000, ideal system
(c) M=172, Number of photons per sampling= 500, DR system
Images are composed of 128 x 128 pixels.

As can be seen, an image from 500 photons per sampling appears to be poorer than that from 1,000 photons per sampling. This result would be the same even for an ideal system for the same amount of injected radionuclides.

Conclusion

The proposed Dichotomic-Ring system has the capability of data collection which leads to reconstruction of images equivalent to an ideal system. Furthermore, it uses much simpler motion than Wobbling and Positology so far proposed for obtaining high resolution images.

Noise optimization and elimination can be made through Wiener fillter approaches as proposed by Cho & Burger,[11] Tsui and Budinger,[12] or Yum.[13]

References

1. G.L. Brownell, W.H. Seet, "Localization of Brain Tumors with Positron Emitters", Nucleonics 11, pp. 40, 1953.
2. S. Rankowitz, J.S. Robertson, W.A. Higibotan et al., "Positron Scanner for Locating Brain Tumors", IRE Int. Conv. Red. 10, No. 9, pp. 49-56, 1962.
3. D.E. Kuhl, K.Q. Edwards, "Image Separation Radioisotopes Scanning" Radiology 80, pp. 653-661, 1963.
4. G.N. Hounsfield, U.K. Pat. No. 1283915, "A Method of and Apparatus for Examination of a Body by Radiation such as X-ray or Gamma Radiation", London, 1972.
5. M.M. Ter-Pogossian, M.E. Phelps, E.J. Hoffman, et al., "Application of Annihilation Coincidence Detection of the Transaxial Reconstruction Tomography", J. Nucl. Med. 16, pp. 210, 1975.
6. Z.H. Cho, J.K. Chan, L. Eriksson, "Circular Ring Transverse Axial Positron Camera for 3-Dimensional Reconstruction of Radionuclides Distribution", IEEE Trans. on Nucl. Sci., NS-23, pp. 613-622, Feb. 1976.
7. R.A. Brooks, V.J. Sank, S.J. Talbert, G. Dichiro, "Sampling Requirements and Detector Motion for Positron Emission Tomographs", IEEE Trans. on Nucl. Sci. NS-26, pp. 2760-2763, Apr. 1979.
8. Chr. Bohm, L. Eriksson, M. Bergstrom, L. Litton, R. Sundan, M. Singh, "A Computer Assisted Ring – Detector Positron Camera System for Reconstruction Tomography of the Brain", IEEE Trans. on Nucl. Sci., NS-25, pp. 624-637, Feb. 1978.
9. M.M. Ter-pogossian, N.A. Mullani, J.T. Hood, C.S. Higgins, D.C. Ficke, "Design Consideration for a Positron Emission Transverse Tomograph (PETT V) for the Imaging of the Brain", J. Comp. Assist. Tomogr., 2, pp. 539-544, Nov. 1978.
10. E. Tanaka, N. Nohara, M. Yamamoto, T. Tomitani, H. Murayama, K. Ishimatsu, K. Takami, "Positology – The Search for Suitable Dectector Arrangements for a Positron ECT with Continuous Rotation", IEEE Transaction on Nucl. Sci., NS-26, pp. 2728-2731, Apr. 1979.
11. Z.H. Cho, J. Burger, "Construction, Restoration, and Enhancement of 2-D and 3-D images", IEEE Trans. on Nucl. Sci., NS-24, No. 2, Apr. 1977.
12. E.T. Tsui, T.F. Budinger, "A Stochastic Filter for Transverse Section Reconstruction", IEEE Trans. on Nucl. Sci. NS-26, pp. 2687-2690, Apr. 1979.
13. Y.H. Yum, to be published.

Appendix
Program Listings

* Common Variables

- M ; Number of projection data per each view
- N ; Number of views
- NX ; Number of pixels per each reconstructed line
- NY ; Number of reconstructed lines
- PROJ ; Generated projection data
- Z ; Pixel values of reconstructed image

A. Projection Data Generation

This program is quoted from Shepp's program

```
*  Input variables
   NLUMPS ; Number of ellipses
   XL, YL ; Center position of ellipse
   AL, BL ; Major and minor axes of ellipse
   TL     ; Tilt of ellipse with respect to vertical axis
   GL     ; Grey level of ellipse
C  PROJ DATA GENERATION(2D)
   DIMENSION XL(11), YL(11), AL(11), BL(11), FACTOR(11), DISTL(11)
   DIMENSION PROJ(256), E(11), GL(11), TL(11)
   CALL OPEN (3, "RJTDDT" 0, IER)
   CALL OPEN (5, "RJCTDT", 0, IER)
   ACCEPT "M = ",M, "N = ",N
   A = 2./M
   PI= 3.14159265
   ACCEPT "NLUMPS= ", NLUMPS
   PIN = PI/N
   DO 10 L= 1,NLUMPS
   READ(5) XL(L), YL(L), AL(L), BL(L), TL(L), GL(L)
   FACTOR(L) = 2.*(AL(L)*BL(L))*GL(L)
10 CONTINUE
   DO 20 J = 1,N
   THE = (J-1)*PIN
   CT = COS(THE)
   ST = SIN(THE)
   DO 30 L = 1, NLUMPS
   S = SIN(THE-TL(L)*PI)
   C = COS(THE-TL(L)*PI)
   E(L) = (AL(L)*C)**2+(BL(L)*S)**2
   DISTL(L) = XL(L)*CT+YL(L)*ST
30 CONTINUE
   DO 40 K = 1,M
   PROJ(L) =0.
40 CONTINUE
   DO 50 K = 1, M
   DO 60 L = 1, NLUMPS
   T = -1. + (K-.5)*A-DISTL(L)
   DIFF = E(L)-T*T
   IF(DIFF.FE.0.) GO TO 60
   PROJ(K) = PROJ(K) + SQRT(DIFF)*FACTOR(L)/E(L)
60 CONTINUE
50 CONTINUE
   WRITE(3,2) (PROJ(I), I = 1,M)
2  FORMAT (1X, 10F7.5)
20 CONTINUE
   STOP
   END
```

B. Reconstruction program

```
O  RECONSTRUCTION ALGORITHM WITH PROPOSED FILTER
   DIMENSION PHI(256), PROJ(256), CONV(256), Z(128, 128)
   CALL OPEN (4, "RJSLAMA", 0, IER)
   CALL OPEN (3, "RJTDDT", 0, IER)
   ACCEPT "M = ", M, "N=", N
   ACCEPT "NX = ", NX, "NY = ", NY
   A = 2./M
   XPOS = 1.-A/2.
   YPOS = XPOS
   PI = 3.14159265
   PIN = PI/N
   C2 = -1./(2.*PI*A*N)
   DELTA = 2.*XPOS/NX
   PHI(L) = 2./(PI*A*N)
   DO 10 K = 2,M
   PHI(K) = C2/((K-1)*(K-1) -.25)
10 CONTINUE
   DO 15 J=1, NY
   DO 15 I = 1,NX
   Z (I, J) = 0.
15 CONTINUE
   DO 20 J = 1, N
   THETAJ = (J-1)*PIN
   ACOSTJ = COS(THETAJ)
   ASINTJ = SIN(THETAJ)
   ACSDEL = ACOSTJ*DELTA/A
   READ(3, 2) (PROJ(I), I = 1,M)
2  FORMAT (10F7.5)
   DO 30 KR = 1, M
   CONV(KR) = 0.
   DO 40 K = 1, M
   KABS = IABS(KR-K)+1
```

```
      CONV(KR) = CONV(KR) + PROJ(K)
       *PHI(KABS)
   40 CONTINUE
   30 CONTINUE
      DO 51 IY = 1, NY
      ZIY = NX*IY/(NY+1.)
      YI = YPOS*(-1.+2.*ZIY/NX)
      R  = (-XPOS*ACOSTJ+ASINTJ*YI+1.)/
       A-ACSDEL+.5
      DO 50 I = 1,NX
      R = R + ACSDEL
      L = R
      IF ((L,LE.0).OR.(L.GE.M)) GO TO 50
      Z(I, IY) = Z(I, IY) + (L + 1 - R)*CONV(L)
       +(R-L)*CONV(L+1)
   50 CONTINUE
   51 CONTINUE
   20 CONTINUE
      DO 60 J = 1, NY
      WRITE(4, 1) (Z(I, J), I = 1,NX)
    1 FORMAT (1X, 5E13.6)
   60 CONTINUE
      STOP
      END
```